Desalination and Water Treatment
www.deswater.com
doi: 10.5004/dwt.2023.29756

306 (2023) 63–74
September

Optimization of heavy metals removal from wastewater by magnetic nano-zeolite using response surface methodology

Hassan A. Shamkhi[a], Maryam Jawad Abdulhasan[a,b,*], Shahad A. Raheem[c], Hussein A.M. Al-Zubaidi[d], Amjed Sabah Kamil Janabi[e]

[a]*Chemical Engineering and Petroleum Industries Department, Al-Mustaqbal University College, Babylon, Iraq, emails: maryam.jawad@uomus.edu.iq (M.J. Abdulhasan), hassan.ali@uomus.edu.iq (H.A. Shamkhi)*
[b]*Ministry of Environment, Department of Protection and Improvement of the Environment in Middle Euphrates Region, Directorate of Babylon Environment, Babylon, Iraq, email: mm893505@gmail.com*
[c]*Hydraulic Structures Engineering Department, College Engineering, Al-Qasim Green University, Babylon, Iraq, email: shahad.ak@wrec.uoqasim.edu.iq*
[d]*Department of Environmental Engineering, Faculty of Engineering, University of Babylon, Iraq, email: hussein.alzubaidi@uobabylon.edu.iq*
[e]*Republic of Iraq Ministry of Construction and Housing, Municipalities and Public Works, Baghdad, Iraq, email: msc.amj89ed@gmail.com*

Received 14 January 2023; Accepted 9 July 2023

ABSTRACT

Response surface methodology (RSM) has been utilized to analyze and optimize sensitive parameters that can affect the reliability of removal processes. This paper aimed to utilize magnetic nano-zeolite (MNZ) as an adsorbent to remove heavy metals, mainly cadmium (Cd(II)) and copper (Cu(II)) ions, from wastewater. Field-emission scanning electron microscopy, zeta potential, and energy-dispersive X-ray spectroscopy were used to characterize the MNZ. The results showed that the maximum removal ratio for cadmium (Cd(II)) was 93%, and for copper (Cu(II)) was 94.5% at optimal conditions of a 68-min run time, pH of 6.5, MNZ of 0.3 mg/L, Cd(II) and Cu(II) concentrations of 50 ppm, and shaking speed of 233 rpm. The model-predicted responses also showed good agreement with actual data (R^2 = 0.9986 for Cd(II), 0.9976 for Cu(II)), demonstrating the effectiveness of this approach for making precise predictions. The adsorption using MNZ was better than that using natural zeolite due to its high cation exchange capacity and large surface area.

Keywords: Magnetic nano-zeolite; Cd(II) removal; Cu(II) removal; RSM; Treatment; Wastewater

1. Introduction

Wastewater is a major source of toxic metals, such as cadmium, lead, zinc, chromium, and mercury, which have a significant impact on water bodies [1–4]. When the concentration of heavy metals exceeds allowable limits, it can pose risks to human health. Even when the metal content is below these limits, long-term contamination remains a concern. These persistent and non-biodegradable metals pose serious hazards to human health and can accumulate in the environment, including the food chain [5–8].

Various techniques are available for removing toxic metals from solutions, including chemical oxidation [9], membrane separation [10], coagulation [11], ion exchange [12], and adsorption [13,14]. Among these techniques, adsorption using zeolite has proven to be a successful and economical

* Corresponding author.

method [5]. Zeolite adsorption has been widely used for pollutant removal due to its high efficiency [15–17]. The adsorption process by zeolites is influenced by factors such as the polarity of the target analytes, accessible surface area, and zeolite size [18]. In recent years, the green production of nanoparticles has gained popularity due to its numerous benefits, including affordability, simplicity, and the absence of stabilizers and hazardous compounds [19–22].

Response surface methodology (RSM), a design of experiments, has been effectively utilized in various processes, particularly in wastewater treatment, for optimizing variables. RSM encompasses different types, such as Box–Behnken design (BBD), face-centered composite design (FCCD), and central composite design (CCD) [23]. RSM offers advantages over conventional techniques by minimizing experimental runs, providing sufficient data for statistically accurate conclusions, and evaluating the significance of parameters and their interactions. Compared to other studied, BBD is an effective RSM method that requires fewer experimental runs and finds extensive application in industrial research [24]. In a study on Pb(II) and Cd(II) removal using clinoptilolite zeolite as an adsorbent, RSM was employed for optimization and analysis, resulting in a maximum removal ratio achieved at pH 6.6, adsorbent amount of 0.19 g, pollutant concentration of 10 ppm, and run time of 22 min [25]. Another study utilized zeolite powder for ammonia removal, demonstrating good adsorption performance with rapid adsorption rates and equilibrium reached within 10 min. Temperature had a minimal effect on adsorption efficiency between 10°C–60°C, and zeolite adsorption of ammonia nitrogen followed the Freundlich isotherm [26]. Natural clinoptilolite zeolite was evaluated for the removal of chromium(III), copper(II), and iron(III) from wastewater, showing high effectiveness with removal percentages of 85.1% for chromium, 95.4% for iron, and 96.0% for copper at pH 4 and 25°C [27].

This paper focuses on the synthesis of magnetic nano-zeolite (MNZ) as an affordable adsorbent. The physico-chemical properties of the synthesized adsorbent, including zeta potential, chemical composition, and morphology, were characterized. RSM was utilized to optimize the adsorbent quantity, contaminant concentration, run time, and pH for removal conditions. Furthermore, the effectiveness of the adsorbent in wastewater samples and its reusability were examined.

2. Materials and methods

2.1. Contaminants preparation

Copper nitrate ($Cu(NO_3)_2$) with a purity of at least 99.00% and cadmium ($Cd(NO_3)_2{\cdot}2H_2O$) with a purity of at least 99.9% were selected as the representative heavy metal contaminants in this research. A total of 1.5985 g of $Cu(NO_3)_2$ was dissolved in 1,000 mL of distilled water to create a stock solution, resulting in a water sample with a copper concentration of 1,000 ppm. Similarly, 0.137 g of $Cd(NO_3)_2{\cdot}2H_2O$ was dissolved in 1,000 mL of distilled water to generate a water sample with a cadmium concentration of 50 mg/L.

2.2. Magnetic nano-zeolite preparation

For the preparation of MNZ, a dispersion was created by mixing 1.0 g of natural zeolite obtained from *Pistacia lentiscus* (mastic tree) with 50 mL of plant extract (consisting of resin acid and gum). To this mixture, 0.6 g of $FeCl_3$ in 10 mL of distilled water was added. The dispersion was continuously agitated while a sodium carbonate solution was added to adjust the pH of the mixture to 8. The reaction mixture was then boiled, and the resulting precipitate was heated at 250°C for 1 h in a furnace. Finally, the resultant MNZ was washed several times with distilled water, as shown in Fig. 1. This method is in agreement with [28].

2.3. Field-emission scanning electron microscopy analysis

FESEM (field emission scanning electron microscopy) is a magnification tool used to scan and capture images of a sample, providing insights into its surface appearance and composition [29]. It is particularly useful for studying the surface of MNZ. The size and shape of MNZ crystals were

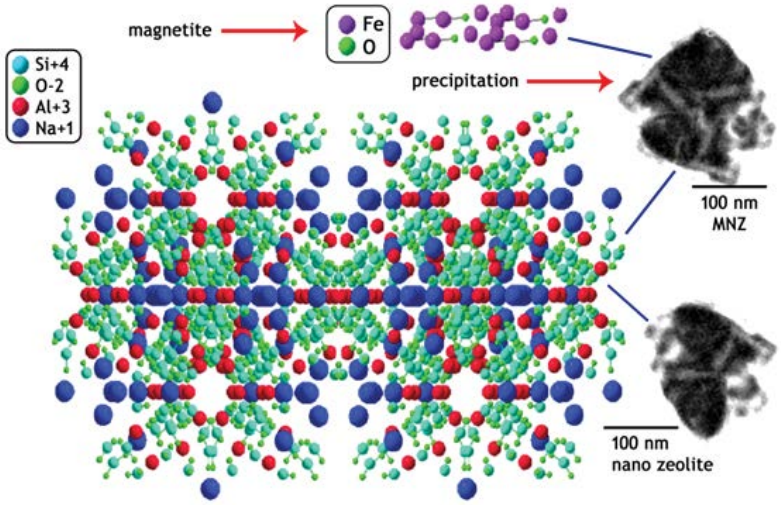

Fig. 1. Image of magnetic nano-zeolite preparation.

determined using scanning electron microscopy images, which revealed the nanostructural characteristics of MNZ materials. Photographs taken at magnifications ranging from 1,000X to 3,000X showed that the MNZ sample is composed of fine-grained material with a lamellar texture and extensive structural damage, as depicted in Fig. 2.

2.4. Energy-dispersive X-ray spectroscopy

The EDXS (energy-dispersive x-ray spectroscopy) spectrum of the MNZ is presented in Fig. 3. Based on the EDXS analysis, the nanocomposite consists of various components, including silicon, iron (Fe), aluminum (Al), carbon (C), and oxygen (O).

2.5. Zeta potential analysis

Zeta potential analysis was employed to assess the surface charge of MNZ, which ranged from 150 to 150 mV. When the zeta potential shifted to 34.6 mV, it indicated that the surface of MNZ maintained a negative charge throughout the entire study period.

2.6. RSM experimental design

The responses of the adsorption system, specifically the percentage of Cd removal (% Cd re.) and the percentage of Cu removal (% Cu re.), were correlated with the influencing variables of the process using the mathematical-statistical tools and mathematical models provided by the RSM method [30,31].

The factors influencing the removal of Cu(II) and Cd(II) ions from wastewater were investigated and monitored using a 5-factor 3-level Box–Behnken design (BBD). The process parameters considered were time (*A*), pH (*B*), pollutant concentration (*C*), MNZ concentration (*D*), and speed (*E*). The response functions considered were the removal ratio of Cu(II) (% Cu re.) and Cd(II) (% Cd re.).

The process parameters were scaled into a code representing high level (1), middle point (0), and low level (–1). The selected process parameters and their corresponding levels are presented in Table 1. The Box–Behnken design is advantageous as it allows for the use of a reduced number of runs compared to a full factorial design, while still obtaining a suitable quadratic model with desired statistical properties. Second-order response surface models were employed to describe the variations in removal efficiencies (*Y*) of Cd(II) and Cu(II) ions based on the independent factors (*A*, *B*, *C*, *D*, and *E*). Eq. (1) demonstrates how the quadratic model can be utilized to predict removal efficiencies [9,32,33].

$$Y = \beta_0 + \sum_{i=1}^{k} \beta_i X_i + \sum_{j=1}^{k} \beta_j X_j^2 + \sum_{i=1}^{k} \sum_{j=2}^{k} \beta_{ij} X_i X_j \quad (1)$$

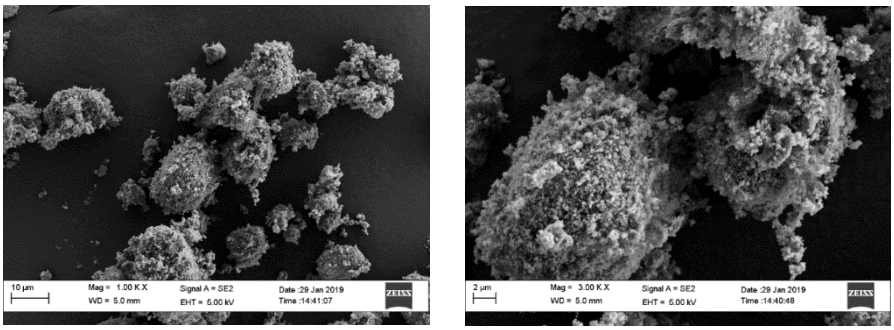

Fig. 2. Scanning electron microscopy images of MNZ.

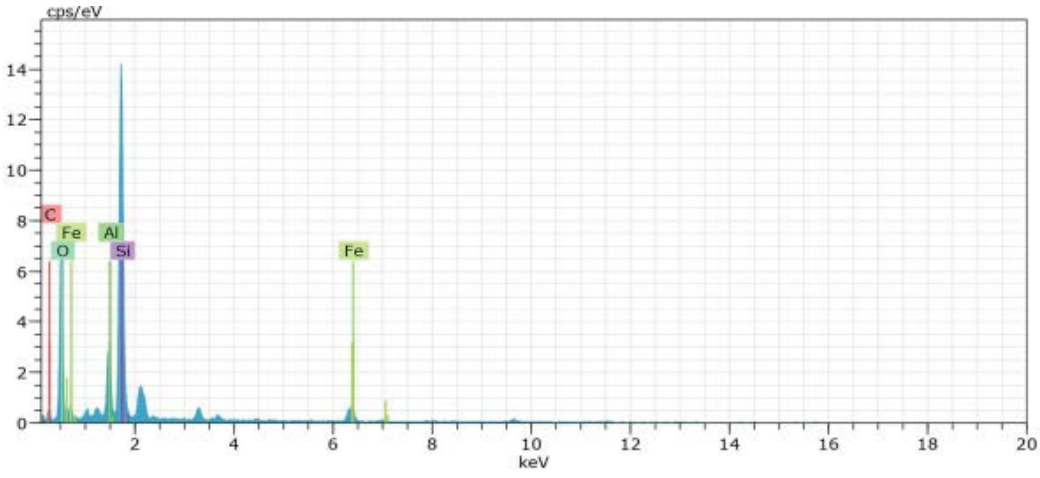

Fig. 3. Energy-dispersive X-ray spectrum for the MZNC sample along with the abundances of each element.

Table 1
Experimental range and levels of independent process parameters for Box–Behnken design

Parameters	Unit	Symbols	Coded factor levels		
			–1	0	1
Time	min.	*A*	20	60	120
pH	–	*B*	2	5	8
concentration of pollutant	mg/L	*C*	50	150	250
MNZ concentration	g	*D*	0.1	0.55	1
Speed	rpm	*E*	0	125	250

where Y is the predicted of removal efficiency (RE%), k is the number of variables examined in the experiments, β_i, β_j, β_{ij} are the impact coefficients of linear, second-degree, and binary influence on the response, respectively, β_0 is the model intercept coefficient, X_i, X_j are the coded value of every variable. The interaction and main effects plot are used to evaluate the individual effects, fitted model, and interaction of the parameters. Statistical importance was proven by the Fisher's test. To see the individual and combined impacts of the independent factors, as well as the sensitive parameters for the removal of Cd(II) and Cu(II) ions in this study, response surface contour and 3-dimensional (3D) plots were created.

3. Results and discussion

3.1. Experiment results and statistical analysis of RSM

The statistical method known as response surface methodology (RSM) was employed in the experimental design to evaluate the influence of process parameters (independent variables) on one or more response variables (dependent variables). RSM effectively reduces the number of required experiments while taking into account the interactions between the parameters [34,35].

To assess the potential influence of process parameters on the removal ratio of Cd(II) and Cu(II) ions from wastewater, a total of 42 batch runs were conducted in this study, considering different groups of process parameters. The results obtained from these experiments are presented in Table 2. The removal efficiencies of Cd(II) and Cu(II) ions, both experimentally determined and predicted, were reported. A comparison between the experimental and predicted outcomes demonstrated a high level of agreement, as illustrated in Fig. 4.

To establish a correlation between the removal ratio and the process parameters, the removal efficiencies of Cd(II) and Cu(II) ions were analyzed using Design–Expert 13 software. The final quadratic models derived from the analysis are as follows:

Final equation in terms of coded factors of % Cu removal.

$$\begin{aligned}\text{RE\% Cd} = {} & +72.75 + 3.83A + 16.21B - 11.09C - 5.41D \\ & + 12.41E - 3.03AB + 2.50AC + 0AD + 4.53AE \\ & + 5.17BC - 6.72BD + 2.25BE + 0.75CD \\ & - 12.25CE + 1.37DE - 7.95A^2 - 13.25B^2 \\ & - 3.93C^2 - 11.39D^2 - 15.77E^2 \end{aligned} \quad (2)$$

Final equation in terms of coded factors of % Cu removal.

$$\begin{aligned}\text{RE\% Cu} = {} & +77.84 + 3.00A + 13.78B - 10.05C - 6.87D \\ & + 11.86E - 4.16AB + 2.25AC - 1.75AD \\ & + 4.91AE + 3.79BC - 5.91BD + 0.6146BE \\ & - 0.75CD - 12.95CE - 0.0469DE - 8.85A^2 \\ & - 15.96B^2 - 5.03C^2 - 13.87D^2 - 15.48E^2 \end{aligned} \quad (3)$$

where RE% Cd% and RE% Cu are the removal efficiencies of Cd(II) and Cu(II) ions, respectively, (*A*, *B*, *C*, *D*, and *E*) are time, pH, the concentration of pollutant, MNZ concentration, and speed, respectively, *AB*, *AC*, *AD*, *AE*, *BC*, *BD*, *BE*, *CD*, *CE* and *DE* are the interaction effect of the model parameters, and A^2, B^2, C^2, D^2, and E^2 are the quadratic terms of the process parameters.

The positive sign coefficients of Eqs. (2) and (3) mean there is a direct significant impact of processing parameters on the responses such as time and speed, whereas the negative sign coefficients refer to the opposite influence such as concentration of pollutant.

3.2. Analysis of variance

The use of variance sections in conjunction with specific sources of variation allowed for the assessment of the suitability of the Box–Behnken design (BBD) [34]. An analysis of variance (ANOVA) model based on the Fischer *F*-test was conducted to determine the significance of each coefficient. Tables 3 and 4 present the *F*-values and *P*-values for the Cd(II) and Cu(II) ions, respectively. The tables provide information on degrees of freedom (DF), sum of squares (SS), mean square (mean sq.), Fisher-value, and *P*-test value. The *P*-value test is performed to determine if the *F*-value is sufficiently high to demonstrate statistical significance among various statistical parameters. Typically, the significance of a coefficient increases as the *P*-value decreases [36], while the significance of a factor increases with the magnitude of the *F*-value [37,38]. Model terms were considered significant for *P*-values less than 0.05, whereas model terms were deemed insignificant for *P*-values greater than 0.1.

The ANOVA model for the removal of Cd(II) ions from wastewater is presented in Table 4. The statistical significance of the ANOVA model is indicated by its *F*-value of 751.97 and a *P*-value of less than 0.0001. The standard deviation, shown in Table 5, is 0.93. The R^2 value is 0.9986, the R_{adj}^2 value is 0.9983, and the coefficient of variation (C.V.) is 1.71%, indicating an appropriate precision of 111.886. These findings collectively suggest that the model exhibited a high level of reliability in the experiments conducted to select the model.

For the removal of Cu(II) ions, Table 4 presents the corresponding ANOVA model. The statistical significance of the model is demonstrated by its *F*-value of 430.88 and a *P*-value of less than 0.0001. Additionally, Table 5 indicates that the model is highly reliable for copper removal, as evidenced by a standard deviation of 1.13, an R^2 value of 0.9976, a R_{adj}^2 value of 0.9953, a coefficient of variation (C.V.) of 2.04%, and an adequate precision of 88.5746.

Table 2
Experimental design values of response variables for the removal **percentage of** predicted **and** actual **values**

Run	Time	pH	Conc. of pollutant	MNZ conc.	Speed	% Cd removal		% Cu removal	
						Actual value	Predicted value	Actual value	Predicted value
1	120	5	50	0.55	125	73.23	73.29	75.99	74.74
2	70	8	150	0.55	0	44.23	45.27	47.46	47.71
3	20	8	150	0.55	125	68.01	66.97	69.3	67.96
4	70	5	150	0.1	0	40.49	39.97	45.48	43.46
5	120	5	150	0.55	0	36.21	35.92	39.61	39.73
6	70	5	150	1	0	26.79	26.39	30.08	29.81
7	70	8	150	0.55	250	76.06	74.6	73.53	72.65
8	70	2	50	0.55	125	55.73	55.63	56.89	56.89
9	70	8	50	0.55	125	77.81	77.7	76.76	76.88
10	70	2	150	0.1	125	31.13	30.6	35.92	35.2
11	70	5	250	0.55	250	42.35	42.12	46.48	46.19
12	70	2	250	0.55	125	22.58	23.1	29.11	29.23
13	70	2	150	1	125	33.61	33.21	33.24	33.27
14	70	5	50	1	125	61.91	62.36	63.26	62.87
15	70	2	150	0.55	250	38.64	37.68	44.36	43.86
16	70	5	250	0.1	125	51.05	51.01	55.54	56.52
17	70	5	250	0.55	0	42.52	41.79	48.04	48.37
18	70	5	250	1	125	42.1	41.68	43.04	41.27
19	70	5	50	0.55	0	40.33	39.48	42.35	42.56
20	120	5	150	0.55	250	69.09	69.8	72.77	73.27
21	70	5	150	0.55	125	72	72.75	78	77.84
22	120	5	150	1	125	52.31	51.83	49.47	49.5
23	20	5	150	0.55	250	51.88	53.09	56.33	57.46
24	120	2	150	0.55	125	41.75	42.21	45.48	46.39
25	20	5	250	0.55	125	43.27	43.46	48.16	48.66
26	70	8	150	1	125	51.59	52.19	47.87	49.02
27	70	2	150	0.55	0	15.82	17.36	20.75	21.37
28	70	5	50	0.55	250	89.16	88.8	92.6	92.18
29	120	5	250	0.55	125	55.92	56.11	59.28	59.15
30	70	5	50	0.1	125	73.86	74.69	72.75	75.11
31	70	8	150	0.1	125	75.98	76.46	74.17	74.57
32	20	5	150	0.1	125	55.11	55.01	57.35	57.24
33	70	8	250	0.55	125	65.34	65.86	64.11	64.36
34	20	2	150	0.55	125	29.03	28.49	32.55	32.09
35	20	5	50	0.55	125	70.58	70.64	73.88	73.25
36	20	5	150	0.55	0	37.11	37.32	42.81	43.56
37	120	8	150	0.55	125	68.6	68.56	65.6	65.64
38	70	5	150	0.1	250	61.56	62.04	67.92	67.27
39	120	5	150	0.1	125	63.26	62.66	66.97	66.74
40	70	5	150	0.55	125	73.5	72.75	77.68	77.84
41	70	5	150	1	250	53.36	53.97	52.33	53.44
42	20	5	150	1	125	44.16	44.18	46.86	47

3.3. Response surface and contour plots for Cd(II) and Cu(II) ions removal

3.3.1. Initial pH value

The influence of changing the initial pH value from 2 to 8 on MNZ removal was studied under constant conditions (MNZ amount = 0.31 mg/L, concentration of Cd(II) and Cu(II) = 50 mg/L, and shaking speed = 233 rpm), as depicted in Fig. 5. The removal ratio of MNZ was observed to decrease at both low and high pH values. This can be attributed to the ionization states of the substrate and catalyst, where MNZ carries a positive charge at acidic pH

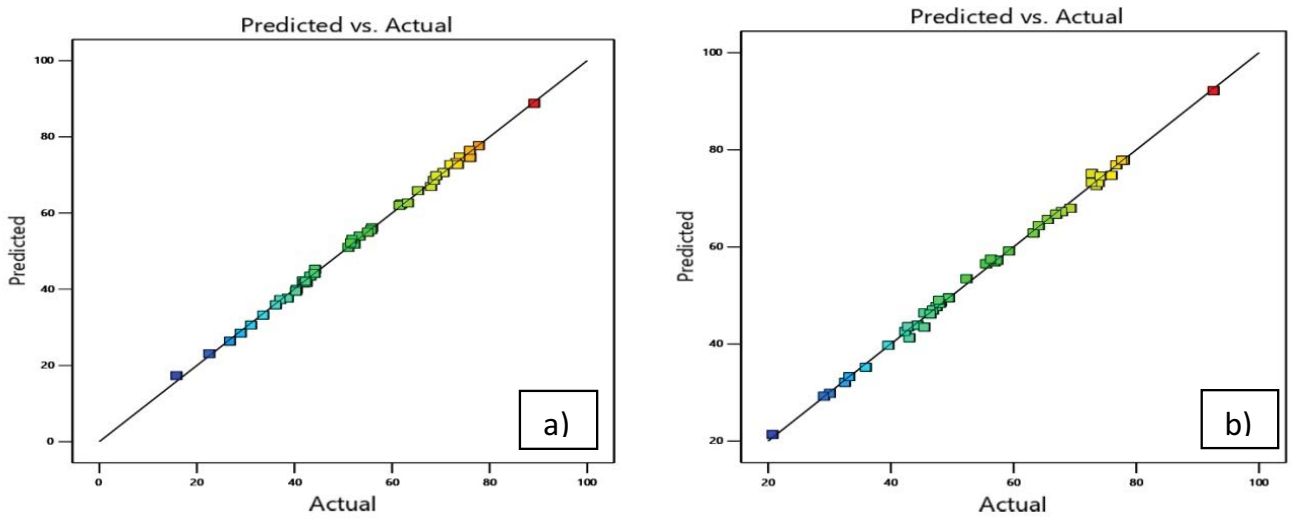

Fig. 4. Plot of predicted vs. actual for (a) % Cd removal and (b) % Cu removal.

Table 3
ANOVA of response surface quadratic model for % Cd removal

Source	Sum of squares	df	Mean square	*F*-value	*P*-value
Model	12,264.16	20	613.21	751.97	<0.0001
A-Time	234.28	1	234.28	287.30	<0.0001
B-pH	4,202.68	1	4,202.68	5,153.69	<0.0001
C-Cd conc.	1,968.68	1	1,968.68	2,414.17	<0.0001
D-MNZ. Conc.	468.99	1	468.99	575.12	<0.0001
E-Speed	2,465.12	1	2,465.12	3,022.95	<0.0001
AB	36.75	1	36.75	45.07	<0.0001
AC	25.00	1	25.00	30.66	<0.0001
AD	0.0000	1	0.0000	0.0000	1.0000
AE	81.90	1	81.90	100.44	<0.0001
BC	106.91	1	106.91	131.10	<0.0001
BD	180.57	1	180.57	221.43	<0.0001
BE	20.25	1	20.25	24.83	<0.0001
CD	2.25	1	2.25	2.76	0.1116
CE	600.25	1	600.25	736.08	<0.0001
DE	7.56	1	7.56	9.27	0.0061
A^2	319.04	1	319.04	391.23	<0.0001
B^2	886.88	1	886.88	1,087.57	<0.0001
C^2	78.01	1	78.01	95.66	<0.0001
D^2	654.93	1	654.93	803.13	<0.0001
E^2	1,256.98	1	1,256.98	1,541.41	<0.0001
Residual	17.12	21	0.8155		
Lack of fit	16.00	20	0.8000	0.7111	0.7504
Pure error	1.13	1	1.13		
Cor. total	12,281.29	41			

and a negative charge at alkaline pH. However, the surface charge of Cd(II) and Cu(II) ions changes from positive to negative. An increase in the removal ratio was observed when the pH increased from 2 to 6.5. This can be explained by the fact that Cd(II) and Cu(II) ions have the same negative charge at alkaline pH as they do at acidic pH. Consequently, the optimal removal was achieved at pH 6.5. These findings are consistent with previous studies [39,40].

Table 4
ANOVA of response surface quadratic model for % Cu removal

Source	Sum of squares	df	Mean square	*F*-value	*P*-value
Model	11,015.28	20	550.76	430.88	<0.0001
A-Time	143.70	1	143.70	112.42	<0.0001
B-pH	3,038.77	1	3,038.77	2,377.31	<0.0001
C-Cu conc.	1,614.70	1	1,614.70	1,263.22	<0.0001
D-MNZ. conc.	755.39	1	755.39	590.96	<0.0001
E-Speed	2,250.02	1	2,250.02	1,760.25	<0.0001
AB	69.10	1	69.10	54.06	<0.0001
AC	20.25	1	20.25	15.84	0.0007
AD	12.25	1	12.25	9.58	0.0055
AE	96.53	1	96.53	75.52	<0.0001
BC	57.32	1	57.32	44.84	<0.0001
BD	139.54	1	139.54	109.16	<0.0001
BE	1.51	1	1.51	1.18	0.2893
CD	2.25	1	2.25	1.76	0.1988
CE	671.03	1	671.03	524.96	<0.0001
DE	0.0088	1	0.0088	0.0069	0.9347
A^2	396.15	1	396.15	309.92	<0.0001
B^2	1,287.49	1	1,287.49	1,007.24	<0.0001
C^2	128.03	1	128.03	100.16	<0.0001
D^2	971.36	1	971.36	759.92	<0.0001
E^2	1,210.65	1	1,210.65	947.12	<0.0001
Residual	26.84	21	1.28		
Lack of fit	26.79	20	1.34	26.16	0.1530
Pure error	0.0512	1	0.0512		
Cor total	11,042.13	41			

Table 5
Summary of regression values for % Cd, % Cu removal

	Std. dev.	Mean	C.V. %	R^2	Adjusted R^2	Predicted R^2	Adeq. precision
% Cd removal	0.9030	52.83	1.71	0.9986	0.9973	0.9944	111.886
% Cu removal	1.13	55.29	2.04	0.9976	0.9953	0.9903	88.5746

3.3.2. Initial concentration of the Cd(II) and Cu(II) ions

In this step, batch studies were conducted with concentrations ranging from 50 to 250 mg/L under the following conditions: contact time of 68.5 min, pH of 3, MNZ dosage of 0.31 mg/L, and shaking speed of 233 rpm. The removal efficiency of Cd(II) and Cu(II) using MNZ as a sorbent was found to be 93% for Cd(II) and 94.5% for Cu(II) at a starting concentration of 50 mg/L, as shown in Fig. 6. This clearly demonstrates the significant influence of concentration on the removal efficiency. Higher pollutant concentrations can result in the occupation of less favorable active sites, leading to a decrease in the amount of pollutant removed. These findings align with previous studies [41,42].

3.3.3. Effect of MNZ value

To investigate the impact of sorbent dosage on the sorption of Cd(II) and Cu(II) ions, the amount of MNZ was varied from 0.1 to 1 g. The batch studies were conducted with a run time of 68.5 min, an initial pH of 6.5, and an agitation speed of 233 rpm. Fig. 7 illustrates how increasing the MNZ weight from 0.1 to 1 g, at a specific starting concentration of 50 mg/L, enhances the efficiency of Cd(II) and Cu(II) removal. This outcome was expected since a higher dosage of the reactive substance would generally provide more binding sites. It indicates that an increased abundance of MNZ leads to a greater number of binding sites available for contaminant removal upon collision with the solute [40].

3.3.4. Agitation speed

Using the optimal conditions determined in previous studies, including a Cd(II) and Cu(II) concentration of 50 mg/L and an MNZ dosage of 0.31 mg/L, with a contact time of 68.5 min and a pH of 6.5, the agitation speed was varied from zero to 233 rpm. Fig. 8 demonstrates that the removal efficiency steadily improved until reaching a value of 93%

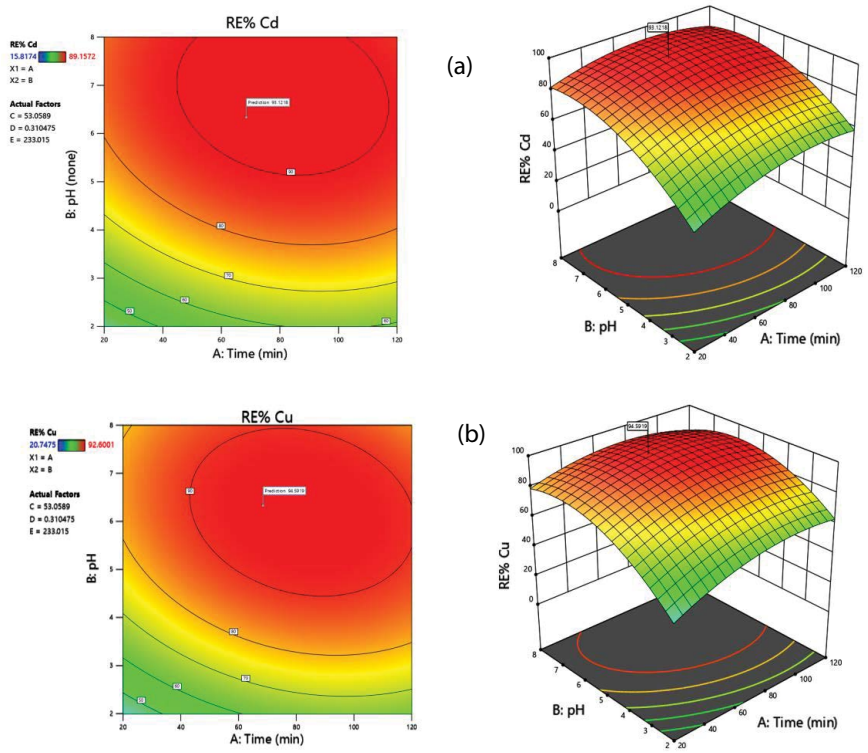

Fig. 5. 3D and 2D plots of initial pH with (a) Cd(II) removal efficiency and (b) Cu(II) removal efficiency.

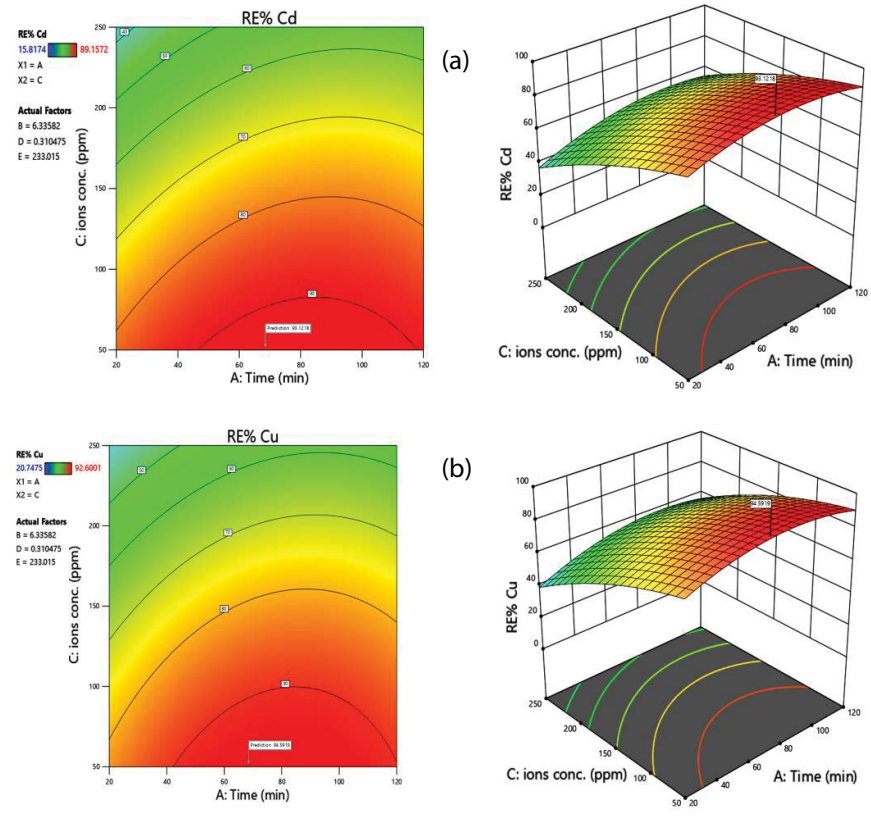

Fig. 6. 3D and 2D plots of initial concentration of Cd(II), Cu(II) with (a) Cd(II) removal efficiency and (b) Cu(II) removal efficiency.

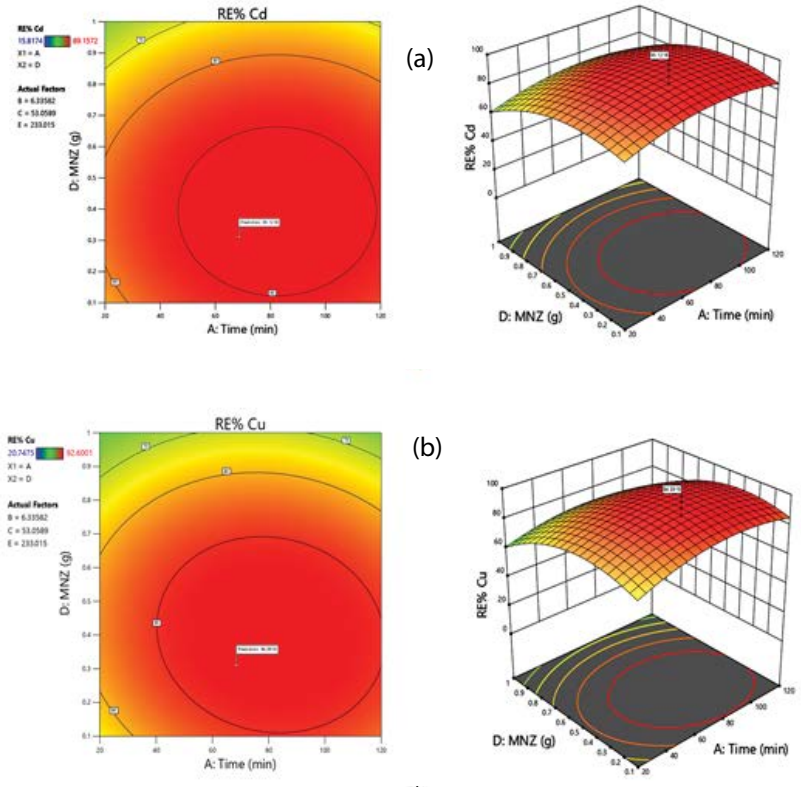

Fig. 7. 3D and 2D plots of MNZ amount with (a) Cd(II) removal efficiency and (b) Cu(II) removal efficiency.

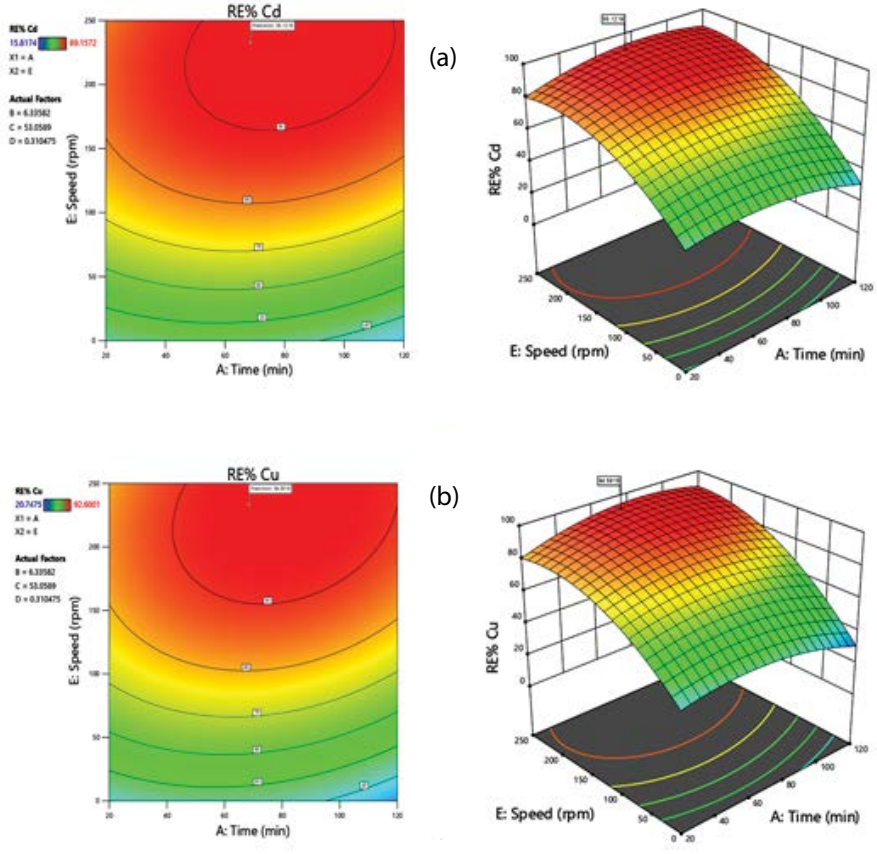

Fig. 8. 3D and 2D plots of shaking speed with (a) Cd(II) removal efficiency and (b) Cu(II) removal efficiency.

Table 6
Process parameters that gave the optimum removal efficiency

Parameters	Time	pH	Conc. of pollutant	MNZ conc.	Speed	% Cd removal	% Cu removal
Optimum value	68.502 min	6.336	53.059 mg/L	0.31 g	233.015 rpm	93.122	94.592

for Cd(II) and 94.5% for Cu(II) at 233 rpm. Approximately 10% of Cd(II) and Cu(II) were eliminated at zero agitation speed. It is evident that an agitation speed of 233 rpm provides appropriate interaction between the active sorbent sites and the contaminant ions in the aqueous solution. This finding is consistent with previous studies [43–45].

3.4. Optimization with RSM

One of the main advantages of using RSM in BBD is its ability to determine the optimal conditions for pollutant removal through laboratory experiments. The regression equation derived from the BBD is used to optimize the results. Design of experiments (DoE) software explores the design space while considering various constraints to improve the process. Multiple random starting points are selected to identify the true maximum and minimum values. Each process variable and response variable should have a defined objective or goal. The goal for the response variable can be within a specific range, target, or minimize/maximize certain parameters [17,46].

Variables can also be set to specific values. In the optimization process, the variables time (*A*), pH (*B*), the concentration of pollutant (*C*), MNZ concentration (*D*), and speed (*E*) were selected to be within certain ranges, and the responses (% Cd Re.) and (% Cu Re.) were maximized. Based on these process variables, the optimal values were determined as follows: Time of 68.502 min, pH of 6.336, concentration of pollutant of 53.059 mg/L, MNZ concentration of 0.31 g, and speed of 233.015 rpm. The corresponding optimal values for (% Cd Re.) and (% Cu Re.) were found to be 93.122% and 94.592%, respectively, as shown in Table 6.

4. Conclusion

In this work, MNZ was successfully synthesized as an adsorbent to optimize the effect of experimental parameters on the removal efficiency of Cd(II) and Cu(II) using RSM. Based on zeta analysis, the produced MZNC exhibited a negative surface charge, which facilitated its ability to bind positively charged ions. The relationship between the removal efficiency (response) and independent variables was established using a second-order polynomial equation based on the experimental results. The removal efficiencies of Cd(II) and Cu(II) were determined to be 93% and 94%, respectively. The optimal conditions for maximum removal efficiency were determined to be a run time of 68 min, pH of 6.5, MNZ dosage of 0.3 mg/L, initial concentrations of Cd(II) and Cu(II) of 50 ppm, and shaking speed of 233 rpm. The model's predicted responses showed a high degree of agreement with the actual data, with R^2 values of 0.9986 for Cd(II) and 0.9976 for Cu(II), indicating the accuracy and precision of the model. The main advantages of this research are the simplicity of MNZ synthesis, its cost-effectiveness, eco-friendliness, and high capacity for removing and binding heavy metals.

Acknowledgements

This work was supported by Al-Mustaqbal University College (grant number MUC-E-0122) and the Department of Environmental Engineering, University of Babylon.

Author contributions

Maryam Jawad Abdulhasan was involved in the study's idea. Maryam Jawad Abdulhasan and Hassan A. Shamkhi wrote the main manuscript. All authors contributed to the preparation of the introduction. Maryam Jawad Abdulhasan and Hassan A. Shamkhi prepared the results and discussion. All authors contributed to the preparation of figures and tables. Maryam Jawad Abdulhasan and Hassan A. Shamkhi prepared the conclusion. All authors reviewed the manuscript.

Conflict of interest

There are no conflicts to declare.

Finding declaration

There are no findings to declare.

Data availability statements

The datasets generated during and/or analyzed during the current study are available from the corresponding author upon reasonable request.

References

[1] N. Jiang, R. Shang, S.G.J. Heijman, L.C. Rietveld, High-silica zeolites for adsorption of organic micro-pollutants in water treatment: a review, Water Res., 144 (2018) 145–161.
[2] E.N. Zare, A. Motahari, M. Sillanpää, Nanoadsorbents based on conducting polymer nanocomposites with main focus on polyaniline and its derivatives for removal of heavy metal ions/dyes: a review, Environ. Res., 162 (2017) 173–195.
[3] S.A. Bhat, T. Hassan, S. Majid, Heavy metal toxicity and their harmful effects on living organisms, Int. J. Med. Sci. Diagn. Res., 3 (2019) 106–122.
[4] H.A. Shamkhia, A.D.Z. Albdiria, Simultaneous extraction of lead, copper, and cadmium from aqueous solution using emulsion liquid membrane technique, Al-Qadisiyah J. Eng. Sci., 13 (2020) 183–188.
[5] R. Arora, Adsorption of heavy metals-a review, Mater. Today Proc., 18 (2019) 4745–4750.
[6] H.A. Shamkhi, A.D.Z. Albdiri, F.A. Jabir, S.S. Koter, Experimental and modeling studies on simultaneous extraction of Pb^{2+}, Cu^{2+},

and Cd^{2+} from diluted acidic aqueous solutions by emulsion liquid membrane, Chem. Eng. Commun., 209 (2022) 246–255.
[7] A. Elhalil, W. Boumya, A. Machrouhi, R. Elmoubarki, S. Mansouri, M. Sadiq, M. Abdennouri, N. Barka, Synthesis, characterization and efficient photocatalytic properties of spinel materials for dye degradation, Appl. Surf. Sci. Adv., 13 (2023) 100381, doi: 10.1016/j.apsadv.2023.100381.
[8] M. El Alouani, S. Alehyen, H. El Hadki, H. Saufi, A. Elhalil, O.K. Kabbaj, M. Taibi, Synergetic influence between adsorption and photodegradation of Rhodamine B using synthesized fly ash based inorganic polymer, Surf. Interfaces, 24 (2021) 101136, doi: 10.1016/j.surfin.2021.101136.
[9] A.S. Fahim, A.H. Abbar, Optimization of process parameters for the electrochemical oxidation treatment of petroleum refinery wastewater using porous graphite anode, Al-Qadisiyah J. Eng. Sci., 13 (2020) 125–135.
[10] S. Hube, M. Eskafi, K.F. Hrafnkelsdóttir, B. Bjarnadóttir, M.Á. Bjarnadóttir, S. Axelsdóttir, B. Wu, Direct membrane filtration for wastewater treatment and resource recovery: a review, Sci. Total Environ., 710 (2020) 136375, doi: 10.1016/j.scitotenv.2019.136375.
[11] C.Y. Teh, P.M. Budiman, K.P.Y. Shak, T.Y. Wu, Recent advancement of coagulation–flocculation and its application in wastewater treatment, Ind. Eng. Chem. Res., 55 (2016) 4363–4389.
[12] H. Khanmohammadi, B. Bayati, J. Rahbar-Shahrouzi, A.-A. Babaluo, A. Ghorbani, Molecular simulation of the ion exchange behavior of Cu^{2+}, Cd^{2+} and Pb^{2+} ions on different zeolites exchanged with sodium, J. Environ. Chem. Eng., 7 (2019) 103040, doi: 10.1016/j.jece.2019.103040.
[13] A.E. Burakov, E.V. Galunin, I.V. Burakova, A.E. Kucherova, S. Agarwal, A.G. Tkachev, V.K. Gupta, Adsorption of heavy metals on conventional and nanostructured materials for wastewater treatment purposes: a review, Ecotoxicol. Environ. Saf., 148 (2018) 702–712.
[14] S. De Gisi, G. Lofrano, M. Grassi, M. Notarnicola, Characteristics and adsorption capacities of low-cost sorbents for wastewater treatment: a review, Sustainable Mater. Technol., 9 (2016) 10–40.
[15] T. Amiri-Yazani, R. Zare-Dorabei, M. Rabbani, A. Mollahosseini, Highly efficient ultrasonic-assisted pre-concentration and simultaneous determination of trace amounts of Pb(II) and Cd(II) ions using modified magnetic natural clinoptilolite zeolite: response surface methodology, Microchem. J., 146 (2018) 498–508.
[16] M.F. Mubarak, A.M.G. Mohamed, M. Keshawy, T.A. elMoghny, N. Shehata, Adsorption of heavy metals and hardness ions from groundwater onto modified zeolite: batch and column studies, Alexandria Eng. J., 61 (2022) 4189–4207.
[17] X. Yang, B. Yan, Y. Liu, F. Zhou, D. Li, Z. Zhang, Gamma-FeOOH based hierarchically porous zeolite monoliths for As(V) removal: characterisation, adsorption and response surface methodology, Microporous Mesoporous Mater., 308 (2020) 110518, doi: 10.1016/j.micromeso.2020.110518.
[18] M. Delkash, B. Ebrazi Bakhshayesh, H. Kazemian, Using zeolitic adsorbents to cleanup special wastewater streams: a review, Microporous Mesoporous Mater., 214 (2015) 224–241.
[19] M. Roni, K. Murugan, C. Panneerselvam, J. Subramaniam, M. Nicoletti, P. Madhiyazhagan, D. Dinesh, U. Suresh, H.F. Khater, H. Wei, A. Canale, A.A. Alarfaj, M.A. Munusamy, A. Higuchi, G. Benelli, Characterization and biotoxicity of *Hypnea musciformis*-synthesized silver nanoparticles as potential eco-friendly control tool against *Aedes aegypti* and *Plutella xylostella*, Ecotoxicol. Environ. Saf., 121 (2015) 31–38.
[20] M. Nasrollahzadeh, S.M. Sajadi, M. Maham, I. Kohsari, Biosynthesis, characterization and catalytic activity of the Pd/bentonite nanocomposite for base- and ligand-free oxidative hydroxylation of phenylboronic acid and reduction of chromium(VI) and nitro compounds, Microporous Mesoporous Mater., 271 (2018) 128–137.
[21] S. Chauhan, L.S.B. Upadhyay, Biosynthesis of iron oxide nanoparticles using plant derivatives of *Lawsonia inermis* (Henna) and its surface modification for biomedical application, Nanotechnol. Environ. Eng., 4 (2019), doi: 10.1007/s41204-019-0055-5.
[22] F.Z. Janani, H. Khiar, N. Taoufik, A. Elhalil, M. Sadiq, A.V. Puga, S. Mansouri, N. Barka, $ZnO–Al_2O_3–CeO_2–Ce_2O_3$ mixed metal oxides as a promising photocatalyst for methyl orange photocatalytic degradation, Mater. Today Chem., 21 (2021) 100495, doi: 10.1016/j.mtchem.2021.100495.
[23] K.A. Mohamad Said, M.A. Mohamed Amin, Overview on the response surface methodology (RSM) in extraction processes, J. Appl. Sci. Process Eng., 2 (2016) 8–17.
[24] K. Elsayed, C. Lacor, Modeling, analysis and optimization of aircyclones using artificial neural network, response surface methodology and CFD simulation approaches, Powder Technol., 212 (2011) 115–133.
[25] X. Sun, R. Abbass, M. Ghoroqi, I. Patra, N.K.A. Dwijendra, K.F. Uktamov, H. Jasem, Optimization of dyes and toxic metals removal from environmental water samples by clinoptilolite zeolite using response surface methodology approach, Sci. Rep., 12 (2022) 13218, doi: 10.1038/s41598-022-17636-8.
[26] J. Wang, W. Jin, H. Guo, X. Wang, J. Liu, Experimental study on ammonia nitrogen adsorption performance of zeolite powder, Chem. Eng. Trans., 46 (2015) 79–84.
[27] E. Zanin, J. Scapinello, M. de Oliveira, C.L. Rambo, F. Franscescon, L. Freitas, J.M.M. de Mello, M.A. Fiori, J. Vladimir Oliveira, J. Dal Magro, Adsorption of heavy metals from wastewater graphic industry using clinoptilolite zeolite as adsorbent, Process Saf. Environ. Prot., 105 (2017) 194–200.
[28] R. Karami-Osboo, M. Maham, M. Nasrollahzadeh, Rapid and sensitive extraction of aflatoxins by Fe_3O_4/zeolite nanocomposite adsorbent in rice samples, Microchem. J., 158 (2020) 105206, doi: 10.1016/j.microc.2020.105206.
[29] K. Ramesh, K. Sammi Reddy, I. Rashmi, A.K. Biswas, Porosity distribution, surface area, and morphology of synthetic potassium zeolites: a SEM and N_2 adsorption study, Commun. Soil Sci. Plant Anal., 45 (2014) 2171–2181.
[30] C. Zhao, S. Shao, Y. Zhou, Y. Yang, Y. Shao, L. Zhang, Y. Zhou, L. Xie, L. Luo, Optimization of flocculation conditions for soluble cadmium removal using the composite flocculant of green anion polyacrylamide and PAC by response surface methodology, Sci. Total Environ., 645 (2018) 267–276.
[31] S.J.S. Chelladurai, K. Murugan, A.P. Ray, M. Upadhyaya, V. Narasimharaj, S. Gnanasekaran, Optimization of process parameters using response surface methodology: a review, Mater. Today Proc., 37 (2020) 1301–1304.
[32] Z.N. Abbas, A.H. Abbar, Application of response surface methodology for optimization of cadmium removal from simulated wastewater using a rotating tubular packed bed electrochemical reactor, Al-Qadisiyah J. Eng. Sci., 13 (2020) 91–98.
[33] I.G. Ezemagu, M.I. Ejimofor, M.C. Menkiti, C.C. Nwobi-Okoye, Modeling and optimization of turbidity removal from produced water using response surface methodology and artificial neural network, S. Afr. J. Chem. Eng., 35 (2021) 78–88.
[34] H.A. Shamkhi, A.D.Z. Albdiri, F.A. Jabir, D. Petruzzelli, Removal of Pb^{2+}, Cu^{2+}, and Cd^{2+} ions from a saline wastewater using emulsion liquid membrane: applying response surface methodology for optimization and data analysis, Arabian J. Sci. Eng., 47 (2022) 5705–5719.
[35] Y.G. Asfaha, A.K. Tekile, F. Zewge, Hybrid process of electrocoagulation and electrooxidation system for wastewater treatment: a review, Cleaner Eng. Technol., 4 (2021) 100261, doi: 10.1016/j.clet.2021.100261.
[36] H. Asadian, A. Ahmadi, The extraction of gallium from chloride solutions by emulsion liquid membrane: optimization through response surface methodology, Miner. Eng., 148 (2020) 106207, doi: 10.1016/j.mineng.2020.106207.
[37] R.G. Najeeb, A.H. Abbar, Optimization of COD removal from pharmaceutical wastewater by electrocoagulation process using response surface methodology (RSM), Egypt. J. Chem., 65 (2022) 619–631.
[38] E. Fathi, P. Gharbani, Modeling and optimization removal of reactive Orange 16 dye using MgO/g-C_3N_4/zeolite nanocomposite in coupling with LED and ultrasound by

response surface methodology, Diamond Relat. Mater., 115 (2021) 108346, doi: 10.1016/j.diamond.2021.108346.
[39] A.H.A. Saad, A.M. Azzam, S.T. El-Wakeel, B.B. Mostafa, M.B. Abd El-latif, Removal of toxic metal ions from wastewater using ZnO@chitosan core-shell nanocomposite, Environ. Nanotechnol. Monit. Manage., 9 (2018) 67–75.
[40] N. Elboughdiri, H. Arellano-Garcia, The use of natural zeolite to remove heavy metals Cu(II), Pb(II) and Cd(II), from industrial wastewater, Cogent Eng., 7 (2020) 1782623, doi: 10.1080/23311916.2020.1782623.
[41] I.V. Joseph, L. Tosheva, A.M. Doyle, Simultaneous removal of Cd(II), Co(II), Cu(II), Pb(II), and Zn(II) ions from aqueous solutions via adsorption on FAU-type zeolites prepared from coal fly ash, J. Environ. Chem. Eng., 8 (2020) 103895, doi: 10.1016/j.jece.2020.103895.
[42] W. Wang, J. Cui, J. Li, J. Du, Y. Chang, J. Cui, X. Liu, X. Fan, D. Yao, Removal effects of different emergent-aquatic-plant groups on Cu, Zn, and Cd compound pollution from simulated swine wastewater, J. Environ. Manage., 296 (2021) 113251, doi: 10.1016/j.jenvman.2021.113251.
[43] M. Ruthiraan, E.C. Abdullah, N.M. Mubarak, M.N. Noraini, A promising route of magnetic based materials for removal of cadmium and methylene blue from waste water, J. Environ. Chem. Eng., 5 (2017) 1447–1455.
[44] M.J. Nasir, M.J. Abdulhasan, S.Z.A. Ridha, K.S. Hashim, H.M. Jasim, Statistical assessment for performance of Al-Mussaib drinking water treatment plant at the year 2020, Water Pract. Technol., 17 (2022) 808–816.
[45] M.J. Abdulhasan, N.J.H. Al-Mansori, M.J. Nasir, Removal turbidity of water by application of electromagnetic field technology, J. Ecol. Eng., 23 (2022) 51–54.
[46] S.A. Raheem, E.J. Kadhim, M.J. Abdulhasan, Comparative study of iron removal from groundwater using low cost adsorbents, J. Ecol. Eng., 23 (2022) 18–23.